

A low-rank multipatch isogeometric method based on Tucker tensors*

M. Montardini ^{†‡}G. Sangalli ^{†‡}M. Tani ^{†‡}

December 15, 2023

Abstract

In this paper we present a low-rank method for conforming multipatch discretizations of compressible linear elasticity problems using Isogeometric Analysis. The proposed technique is a non-trivial extension of [19] to multipatch geometries. We tackle the model problem using an overlapping Schwarz method, where the subdomains can be defined as unions of neighbouring patches. Then on each subdomain we approximate the blocks of the linear system matrix and of the right-hand side vector using Tucker matrices and Tucker vectors, respectively. We use the Truncated Preconditioned Conjugate Gradient as a linear solver, coupled with a suited preconditioner. The numerical experiments show the advantages of this approach in terms of memory storage. Moreover, the number of iterations is robust with respect to the relevant parameters.

1 Introduction

Isogeometric Analysis (IgA) has undergone significant development since the seminal paper [13]. Among other reasons, IgA is interesting as high-order PDEs solver. Indeed, IgA benefits from the approximation properties of splines, which, especially in the case of maximal regularity (splines of continuity C^{p-1} and polynomial degree p), exhibits approximation properties superior to those of classical C^0 or discontinuous piecewise polynomials (see [2]), These approximation properties are very close to optimality in the sense of n-widths (see [9]).

As with all high-order numerical methods, having efficient solvers is fundamental, and this has been a topic of interest and activity in the IgA community. Among the various solutions developed in this regard, low-rank compression techniques have been recently explored, leveraging the tensorial construction of isogeometric spaces on the so-called patch. See, for example, [18, 12, 14, 22], where the authors use a low-rank representation of the isogeometric Galerkin matrices. Low-rank tensor methods have been also exploited in the solution of IgA linear system in [11, 19], based on the Tucker format, and in [3], that uses the tensor-trains approximation of the unknown.

In all these works, a single patch is considered, but clearly the interest lies in multipatch geometries. The extension is not trivial since, obviously, the multipatch setting is not globally tensorial. In this work, we combine a domain decomposition solver with the low-rank technology previously developed in [19]. In particular, we adopt an overlapping Schwarz solver, in the setting of [1], which simplifies communication between patches in the low-rank perspective. The proposed method is tested on some toy problems in the field of linear elasticity, yielding interesting results, particularly in terms of memory compression. This allows for the efficient treatment of multipatch problems with a high number of degrees of freedom.

The paper is organized as follows. In Section 2 we present the basics of IgA and of tensor calculus. The core of the paper is Section 3, where we propose the novel multipatch low-rank strategy. We present some numerical experiments in Section 4 while in the last section we draw some conclusions.

*Version of December 15, 2023

[†]Dipartimento di Matematica, Università degli Studi di Pavia, via Ferrata 5, Pavia, Italy.

[‡]Istituto di Matematica Applicata e Tecnologie Informatiche “E. Magenes” del CNR, via Ferrata 5/a, Pavia, Italy.

Emails: monica.montardini@unipv.it, giancarlo.sangalli@unipv.it, mattia.tani@unipv.it

2 Preliminaries

2.1 B-Splines

Let m and p two positive integers. Then, a knot vector in $[0, 1]$ is a set of non-decreasing points $\Xi := \{\xi_1, \dots, \xi_{m+p+1}\}$. We consider only open knot vectors, i.e. we set $\xi_1 = \dots = \xi_{p+1} = 0$ and $\xi_{m+1} = \dots = \xi_{m+p+1} = 1$. Besides the first and the last, knots can be repeated up to multiplicity p .

Univariate B-splines are piecewise polynomials $\hat{b}_i : [0, 1] \rightarrow \mathbb{R}$ for $i = 1, \dots, m$ of degree p that can be defined from the knot vector Ξ according to Cox-De Boor recursion formulas [5]. We define the mesh-size $h := \max\{|\xi_{i+1} - \xi_i| \mid i = 1, \dots, m+p\}$ and we denote the univariate spline space as

$$\hat{\mathcal{S}}_h^p := \text{span}\{\hat{b}_i \mid i = 1, \dots, m\}.$$

For B-splines properties, we refer to [4]. Multivariate B-splines are defined by tensor product of univariate B-splines. In this paper we focus on three-dimensional problems. Thus, given m_1, m_2, m_3 and p_d positive integers, we introduce for $d = 1, 2, 3$ the open knot vectors $\Xi_d := \{\xi_{1,d}, \dots, \xi_{m_d+p_d+1,d}\}$, the corresponding B-splines \hat{b}_{d,i_d} , $i_d = 1, \dots, m_d$, mesh-sizes h_d and univariate spline spaces $\hat{\mathcal{S}}_{h_d}^{p_d}$. The maximum of the mesh-sizes is denoted as $h := \max\{h_d \mid d = 1, 2, 3\}$. Note that for simplicity we are assuming that all univariate B-splines have the same degree. Multivariate B-splines $\hat{B}_{\mathbf{i}} : [0, 1]^3 \rightarrow \mathbb{R}$ are defined as

$$\hat{B}_{\mathbf{i}}(\underline{\xi}) := \hat{b}_{1,i_1}(\xi_1) \hat{b}_{2,i_2}(\xi_2) \hat{b}_{3,i_3}(\xi_3),$$

where $\mathbf{i} := (i_1, i_2, i_3)$ is a multi-index and $\underline{\xi} = (\xi_1, \xi_2, \xi_3)$. We define the corresponding spline space as

$$\hat{\mathcal{S}}_h^p := \text{span}\left\{\hat{B}_{\mathbf{i}} \mid \text{where } \mathbf{i} := (i_1, i_2, i_3) \text{ and } i_d = 1, \dots, m_d \text{ for } d = 1, 2, 3\right\} = \hat{\mathcal{S}}_{h_1}^{p_1} \otimes \hat{\mathcal{S}}_{h_2}^{p_2} \otimes \hat{\mathcal{S}}_{h_3}^{p_3}.$$

2.2 Isogeometric spaces on a multipatch domain

Let $\Omega \subset \mathbb{R}^3$ represent the computational domain, and we assume that it can be written as the union of \mathcal{N}_{ptc} non-overlapping closed sets, called patches, i.e.

$$\Omega = \bigcup_{i=1}^{\mathcal{N}_{ptc}} \Omega^{(i)}$$

and $\Omega^{(i)} \cap \Omega^{(j)}$ has empty interior for $i \neq j$. Let $\Gamma := \left(\bigcup_{i=1}^{\mathcal{N}_{ptc}} \partial\Omega^{(i)}\right) \setminus \partial\Omega$ denote the union of patch interfaces.

For a fixed $i \in \{1, \dots, \mathcal{N}_{ptc}\}$, we introduce three positive integers $m_1^{(j)}, m_2^{(j)}, m_3^{(j)}$ and three open knot vectors $\Xi_d^{(i)} := \{\xi_{1,d}^{(i)}, \dots, \xi_{m_d^{(i)}+p+1,d}^{(i)}\}$, for $d = 1, 2, 3$, where p is another positive integer which does not depend on i and d . Let $h_d^{(i)}$ denote the mesh size of $\Xi_d^{(i)}$ for $d = 1, 2, 3$. Moreover, we introduce $h := \max\{h_d^{(j)} \mid j = 1, \dots, \mathcal{N}_{ptc}, d = 1, 2, 3\}$. The multivariate spline space associated to each patch is denoted as $\hat{\mathcal{S}}_{ptc}^{(i)}$. We assume that for each patch $\Omega^{(i)}$ there exists a non-singular parametrization $\mathcal{F}_i \in \left[\hat{\mathcal{S}}_{ptc}^{(i)}\right]^3$ whose image is $\Omega^{(i)}$, i.e. $\Omega^{(i)} = \mathcal{F}_i([0, 1]^3)$ and the Jacobian matrix $J_{\mathcal{F}_i}$ is invertible everywhere. A face of a given patch $\Omega^{(i)}$ is the image through \mathcal{F}_i of a face of the unit cube. Similarly, an edge of $\Omega^{(i)}$ is the image through \mathcal{F}_i of an edge of the unit cube.

Let $\partial\Omega_D \subseteq \partial\Omega$, which will represent the portion of $\partial\Omega$ endowed with Dirichlet boundary conditions. We need the following assumption.

Assumption 1. *We assume that $\partial\Omega_D \cap \partial\Omega^{(i)}$ is either an empty set or an entire face of $\Omega^{(i)}$ for $i = 1, \dots, \mathcal{N}_{ptc}$.*

For $i = 1, \dots, \mathcal{N}_{ptc}$, we define $\hat{\mathcal{S}}_{ptc,0}^{(i)} \subset \hat{\mathcal{S}}_{ptc}^{(i)}$ as the space generated by the basis functions of $\hat{\mathcal{S}}_{ptc}^{(i)}$ whose image through $\mathcal{F}^{(i)}$ vanishes on $\partial\Omega_D$. Thanks to Assumption 1, $\hat{\mathcal{S}}_{ptc,0}^{(i)}$ is a tensor product space, i.e.

$$\hat{\mathcal{S}}_{ptc,0}^{(i)} := \hat{\mathcal{S}}_{ptc,1}^{(i)} \otimes \hat{\mathcal{S}}_{ptc,2}^{(i)} \otimes \hat{\mathcal{S}}_{ptc,3}^{(i)},$$

where $\widehat{\mathcal{S}}_{ptc,d}^{(i)} := \text{span} \left\{ \widehat{b}_{d,j}^{(i)} \mid j = 1, \dots, n_{ptc,d}^{(i)} \right\}$ are univariate spline spaces, with $n_{ptc,d}^{(i)} := \dim \left(\widehat{\mathcal{S}}_{ptc,d}^{(i)} \right)$, for $d = 1, 2, 3$. Note that $\dim \left(V_{ptc}^{(i)} \right) = \prod_{d=1}^3 n_{ptc,d}^{(i)} =: n_{ptc}^{(i)}$.

Following the isoparametric concept, we define the local isogeometric space on the i -th patch as

$$V_{ptc}^{(i)} := \left\{ \widehat{v}_h \circ \mathcal{F}_i^{-1} \mid \widehat{v}_h \in \widehat{\mathcal{S}}_{ptc,0}^{(i)} \right\}.$$

Moreover, the isogeometric space over Ω is defined as

$$V_h := \left\{ v \in H^1(\Omega) \mid v|_{\Omega^{(i)}} \in V_{ptc}^{(i)}, i = 1, \dots, \mathcal{N}_{ptc} \right\}. \quad (2.1)$$

Throughout the paper, we assume that the meshes are *conforming* at the patch interfaces (see [13]). Under this assumption, we collect all the basis functions from all local spaces, and then identify those functions whose restriction to the interface Γ assumes the same values and it is not identically zero. The resulting set of functions forms a basis for V_h .

2.3 Model problem

Our model problem is the compressible linear elasticity problem. Let $\partial\Omega = \partial\Omega_D \cup \partial\Omega_N$ with $\partial\Omega_D \cap \partial\Omega_N = \emptyset$ and where $\partial\Omega_D$ is non-empty and satisfies Assumption 1. Let $H_D^1(\Omega) := \{v \in H^1(\Omega) \mid v = 0 \text{ on } \partial\Omega_D\}$. For simplicity, we consider only homogeneous Dirichlet boundary conditions, but the non-homogeneous case can be treated similarly. Then, given $\underline{f} \in [L^2(\Omega)]^3$ and $\underline{g} \in [L^2(\partial\Omega_N)]^3$, we consider the Galerkin problem: find $\underline{u} \in [H_D^1(\Omega)]^3$ such that for all $\underline{v} \in [H_D^1(\Omega)]^3$

$$a(\underline{u}, \underline{v}) = F(\underline{v}),$$

where we define

$$a(\underline{u}, \underline{v}) := 2\mu \int_{\Omega} \varepsilon(\underline{u}) : \varepsilon(\underline{v}) d\mathbf{x} + \lambda \int_{\Omega} (\nabla \cdot \underline{u}) (\nabla \cdot \underline{v}) d\mathbf{x}, \quad (2.2)$$

$$F(\underline{v}) := \int_{\Omega} \underline{f} \cdot \underline{v} d\mathbf{x} + \int_{\partial\Omega_N} \underline{g} \cdot \underline{v} ds, \quad (2.3)$$

$\varepsilon(\underline{v}) := \frac{1}{2} (\nabla \underline{v} + (\nabla \underline{v})^T)$ is the symmetric gradient, while λ and μ denote the material Lamé coefficients, that for simplicity we assume to be constant and such that the Poisson ratio $\frac{\lambda}{2(\mu+\lambda)}$ is larger than 0.5.

The corresponding discrete Galerkin problem that we want to solve is the following: find $\underline{u}_h \in [V_h]^3$ such that

$$a(\underline{u}_h, \underline{v}_h) = F(\underline{v}_h), \quad \text{for all } \underline{v}_h \in [V_h]^3, \quad (2.4)$$

where the space V_h has been defined in (2.1). Note that $[V_h]^3 \subseteq [H_D^1(\Omega)]^3$.

2.4 The Tucker format

Throughout the paper, the entries of a matrix $\mathbf{B} \in \mathbb{R}^{m_1 \times m_2}$ are denoted with $[\mathbf{B}]_{i,j}$, $i = 1, \dots, m_1$, $j = 1, \dots, m_2$. Similarly, the entries of a tensor $\mathfrak{B} \in \mathbb{R}^{m_1 \times m_2 \times m_3}$ are denoted with $[\mathfrak{B}]_{i,j,k}$, $i = 1, \dots, m_1$, $j = 1, \dots, m_2$, $k = 1, \dots, m_3$.

Given $\mathbf{B} \in \mathbb{R}^{m_1 \times m_2}$ and $\mathbf{C} \in \mathbb{R}^{n_1 \times n_2}$, their Kronecker product is defined as

$$\mathbf{B} \otimes \mathbf{C} = \begin{bmatrix} [\mathbf{B}]_{1,1} \mathbf{C} & \dots & [\mathbf{B}]_{1,n} \mathbf{C} \\ \vdots & \ddots & \vdots \\ [\mathbf{B}]_{n,1} \mathbf{C} & \dots & [\mathbf{B}]_{n,n} \mathbf{C} \end{bmatrix} \in \mathbb{R}^{m_1 n_1 \times m_2 n_2}.$$

The notion of Kronecker product can be generalized to tensors of higher dimensions. In particular, given $\mathfrak{B} \in \mathbb{R}^{m_1 \times m_2 \times m_3}$ and $\mathfrak{C} \in \mathbb{R}^{n_1 \times n_2 \times n_3}$, their Kronecker product is the tensor of $\mathbb{R}^{m_1 n_1 \times m_2 n_2 \times m_3 n_3}$ whose entries are

$$[\mathfrak{B} \otimes \mathfrak{C}]_{k_1, k_2, k_3} = [\mathfrak{B}]_{i_1, i_2, i_3} [\mathfrak{C}]_{j_1, j_2, j_3} \quad \text{with} \quad k_d = j_d + (i_d - 1)n_d \quad \text{for} \quad d = 1, 2, 3.$$

In this paper we adopt the notation of [20] and say that a vector $\mathbf{v} \in \mathbb{R}^{n_1 n_2 n_3}$ is in Tucker format (or that it is a Tucker vector) when it is written as

$$\mathbf{v} = \sum_{r_1=1}^{R_1^v} \sum_{r_2=1}^{R_2^v} \sum_{r_3=1}^{R_3^v} [\mathbf{v}]_{r_1, r_2, r_3} v_{(1, r_1)} \otimes v_{(2, r_2)} \otimes v_{(3, r_3)}, \quad (2.5)$$

where $v_{(d, r_d)} \in \mathbb{R}^{n_d}$ for $d = 1, 2, 3$ and $r_d = 1, \dots, R_d^v$, while $\mathbf{v} \in \mathbb{R}^{R_1^v \times R_2^v \times R_3^v}$ is called the core tensor of \mathbf{v} . Here the triplet (R_1^v, R_2^v, R_3^v) is referred to as the multilinear rank of \mathbf{v} . Note that $\mathbf{v} \in \mathbb{R}^{n_1 n_2 n_3}$, and the memory required to store it as a Tucker vector is $R_1^v R_2^v R_3^v + R_1^v n_1 + R_2^v n_2 + R_3^v n_3$. This can be significantly lower than the standard $n_1 n_2 n_3$, provided that $R_d^v \ll n_d$, for $d = 1, 2, 3$.

Similarly, we say that a matrix $\mathbf{B} \in \mathbb{R}^{m_1 m_2 m_3 \times n_1 n_2 n_3}$ is in Tucker format (or that it is a Tucker matrix) when it is written as

$$\mathbf{B} = \sum_{r_1=1}^{R_1^B} \sum_{r_2=1}^{R_2^B} \sum_{r_3=1}^{R_3^B} [\mathfrak{B}]_{r_1, r_2, r_3} B_{(1, r_1)} \otimes B_{(2, r_2)} \otimes B_{(3, r_3)}, \quad (2.6)$$

where $B_{(d, r_d)} \in \mathbb{R}^{m_d \times n_d}$ for $d = 1, 2, 3$, $r_d = 1, \dots, R_d^B$, and $\mathfrak{B} \in \mathbb{R}^{R_1^B \times R_2^B \times R_3^B}$.

The matrix-vector product between a Tucker matrix \mathbf{B} as in (2.6) and a Tucker vector \mathbf{v} as in (2.5) can be efficiently computed since

$$\begin{aligned} \mathbf{B}\mathbf{v} &= \sum_{r'_1, r'_2, r'_3} \sum_{r''_1, r''_2, r''_3} [\mathfrak{B}]_{r'_1, r'_2, r'_3} [\mathbf{v}]_{r''_1, r''_2, r''_3} \left(B_{(1, r'_1)} v_{(1, r''_1)} \right) \otimes \left(B_{(2, r'_2)} v_{(1, r''_2)} \right) \otimes \left(B_{(3, r'_3)} v_{(1, r''_3)} \right) \\ &= \sum_{r_1=1}^{R_1^B} \sum_{r_2=1}^{R_2^B} \sum_{r_3=1}^{R_3^B} [\mathfrak{B} \otimes \mathfrak{C}]_{r_1, r_2, r_3} \left(B_{(1, r'_1)} v_{(1, r''_1)} \right) \otimes \left(B_{(2, r'_2)} v_{(1, r''_2)} \right) \otimes \left(B_{(3, r'_3)} v_{(1, r''_3)} \right) \end{aligned}$$

where, in the last line, r'_d and r''_d satisfy $r_d = r'_d + (r''_d - 1)n_d$, for $d = 1, 2, 3$. Note that $\mathbf{B}\mathbf{v}$ is still a Tucker vector with multilinear rank $(R_1^B R_1^v, R_2^B R_2^v, R_3^B R_3^v)$.

Another operation where the Tucker structure can be exploited is the scalar product. Let \mathbf{v} as in (2.5) and let

$$\mathbf{w} = \sum_{r_1=1}^{R_1^w} \sum_{r_2=1}^{R_2^w} \sum_{r_3=1}^{R_3^w} [\mathbf{w}]_{r_1, r_2, r_3} w_{(1, r_1)} \otimes w_{(2, r_2)} \otimes w_{(3, r_3)}, \quad (2.7)$$

where $w_{(d, r_d)} \in \mathbb{R}^{n_d}$ for $d = 1, 2, 3$ and $r_d = 1, \dots, R_d^w$. Then

$$\mathbf{v} \cdot \mathbf{w} = \sum_{r_1} \cdots \sum_{r'_3} [\mathbf{v}]_{r_1, r_2, r_3} [\mathbf{w}]_{r'_1, r'_2, r'_3} \prod_{d=1}^3 v_{(d, r_d)} \cdot w_{(d, r'_d)}$$

The sum between two Tucker vectors is still a Tucker vector with multilinear rank equal to the sum of the multilinear ranks of the addends. Precisely, let \mathbf{v} as in (2.5) and \mathbf{w} as in (2.7). Then

$$\mathbf{z} = \mathbf{v} + \mathbf{w} = \sum_{r_1=1}^{R_1^v + R_1^w} \sum_{r_2=1}^{R_2^v + R_2^w} \sum_{r_3=1}^{R_3^v + R_3^w} \mathfrak{z}_{r_1, r_2, r_3} z_{(1, r_1)} \otimes z_{(2, r_2)} \otimes z_{(3, r_3)},$$

where

$$z_{(d, r_d)} = \begin{cases} v_{(d, r_d)} & \text{for } r_d = 1, \dots, R_d^v \\ w_{(d, r_d - R_d^v)} & \text{for } r_d = R_d^v + 1, \dots, R_d^v + R_d^w \end{cases}, \quad d = 1, 2, 3,$$

and where the core tensor \mathfrak{z} is a block diagonal tensor defined by concatenating the core tensors of \mathbf{v} and \mathbf{w} .

3 Low-rank multipatch method

We introduce another subdivision of the computational domain, namely

$$\Omega = \bigcup_{i=1}^{\mathcal{N}_{sub}} \Theta^{(i)}.$$

Here, differently from the patches defined in Section 2.2, the subdomains $\Theta^{(j)}$ are allowed to overlap, i.e. the intersection of two different subdomains can have a non-empty interior.

We denote with $V_{sub}^{(i)}$ the subspace of V_h whose functions vanish outside $\Theta^{(i)}$, i.e.

$$V_{sub}^{(i)} = \left\{ v_h \in V_h \mid v_h = 0 \text{ on } \Omega \setminus \Theta^{(i)} \right\}.$$

As a basis for $V_{sub}^{(i)}$, we choose the set of basis functions of V_h whose support is included in $\Theta^{(i)}$. A crucial assumption is that each space $V_{sub}^{(i)}$ can be written as (the pushforward of) a tensor product spline space. Precisely, we assume that

$$V_{sub}^{(i)} = \left\{ \hat{v}_h \circ \mathcal{G}_i^{-1} \mid \hat{v}_h \in \widehat{\mathcal{S}}_{sub,0}^{(i)} \right\}, \quad (3.1)$$

where $\mathcal{G}_i : [0, 1]^3 \rightarrow \Theta^{(i)}$ is a non-singular and differentiable map, while

$$\widehat{\mathcal{S}}_{sub,0}^{(i)} = \widehat{\mathcal{S}}_{sub,1}^{(i)} \otimes \widehat{\mathcal{S}}_{sub,2}^{(i)} \otimes \widehat{\mathcal{S}}_{sub,3}^{(i)} \quad (3.2)$$

is a tensor product spline space. Here $\widehat{\mathcal{S}}_{sub,d}^{(i)}$, $d = 1, 2, 3$, represent univariate spline spaces, whose dimension is denoted with $n_{sub,d}^{(i)}$. Note that $\dim(V_{sub}^{(i)}) = \prod_{d=1}^3 n_{sub,d}^{(i)} =: n_{sub}^{(i)}$.

In the setting described in Section 2.2, the subdomains $\Theta^{(i)}$ and the corresponding spaces $V_{sub}^{(i)}$ satisfying (3.1) can be obtained by merging pairs of isogeometric patches and the corresponding spaces. We give details for this construction in Section 3.4.

3.1 The linear system

We split the solution $\underline{u}_h \in [V_h]^3$ of the Galerkin problem (2.4) as

$$\underline{u}_h = \sum_j^{\mathcal{N}_{sub}} \underline{u}_h^{(j)}, \quad \underline{u}_h^{(j)} \in [V_{sub}^{(j)}]^3.$$

Because of the overlap between the subdomains, the subspaces $[V_{sub}^{(1)}]^3, \dots, [V_{sub}^{(\mathcal{N}_{sub})}]^3$ may not be in direct sum and thus the functions $\underline{u}_h^{(1)}, \dots, \underline{u}_h^{(\mathcal{N}_{sub})}$ are not uniquely determined.

We consider the same splitting for the test functions, and on each space $[V_{sub}^{(j)}]^3$ we naturally choose as basis the set

$$\left\{ \underline{e}_k B_i^{(j)} \mid B_i^{(j)} \text{ basis function for } V_{sub}^{(j)}, k = 1, 2, 3 \right\},$$

where \underline{e}_k is the k -th vector of the canonical basis of \mathbb{R}^3 , $k = 1, 2, 3$. Then the discrete Galerkin problem (2.4) is equivalent to the following linear system:

$$\mathbf{A} \mathbf{u} = \begin{bmatrix} \mathbf{A}^{(1,1)} & \dots & \mathbf{A}^{(1,\mathcal{N}_{sub})} \\ \vdots & & \vdots \\ \mathbf{A}^{(\mathcal{N}_{sub},1)} & \dots & \mathbf{A}^{(\mathcal{N}_{sub},\mathcal{N}_{sub})} \end{bmatrix} \begin{bmatrix} \mathbf{u}^{(1)} \\ \vdots \\ \mathbf{u}^{(\mathcal{N}_{sub})} \end{bmatrix} = \begin{bmatrix} \mathbf{f}^{(1)} \\ \vdots \\ \mathbf{f}^{(\mathcal{N}_{sub})} \end{bmatrix} = \mathbf{f}, \quad (3.3)$$

where, for $i, j = 1, \dots, \mathcal{N}_{sub}$, $\mathbf{u}^{(j)}$ is the coordinate vector of $\underline{u}_h^{(j)}$, while $\mathbf{f}^{(i)} \in \mathbb{R}^{3n_{sub}^{(i)}}$ and $\mathbf{A}^{(i,j)} \in \mathbb{R}^{3n_{sub}^{(i)} \times 3n_{sub}^{(j)}}$ are respectively the vector and matrix representations of the functional (2.3) and of the bilinear form (2.2), when considering $[V_{sub}^{(i)}]^3$ as test function space and $[V_{sub}^{(j)}]^3$ as trial function space. Note that the vectorial nature of the basis functions naturally induces a further block structure in $\mathbf{A}^{(i,j)}$ and $\mathbf{f}^{(i)}$:

$$\mathbf{A}^{(i,j)} = \begin{bmatrix} \mathbf{A}^{(i,j,1,1)} & \mathbf{A}^{(i,j,1,2)} & \mathbf{A}^{(i,j,1,3)} \\ \mathbf{A}^{(i,j,2,1)} & \mathbf{A}^{(i,j,2,2)} & \mathbf{A}^{(i,j,2,3)} \\ \mathbf{A}^{(i,j,3,1)} & \mathbf{A}^{(i,j,3,2)} & \mathbf{A}^{(i,j,3,3)} \end{bmatrix}, \quad \mathbf{f}^{(i)} = \begin{bmatrix} \mathbf{f}^{(i,1)} \\ \mathbf{f}^{(i,2)} \\ \mathbf{f}^{(i,3)} \end{bmatrix},$$

with $\mathbf{A}^{(i,j,k,\ell)} \in \mathbb{R}^{n_{sub}^{(i)} \times n_{sub}^{(j)}}$ and $\mathbf{f}^{(i,k)} \in \mathbb{R}^{n_{sub}^{(i)}}$ for $k, \ell = 1, 2, 3$.

The linear system (3.3) may be singular. Nevertheless, it is solvable (as there exists a solution of the Galerkin problem) and since \mathbf{A} is symmetric and positive semidefinite one solution could be found using a Krylov method, such as the Conjugate Gradient method, see [15] and in particular the work in preparation [1].

As a further step, in the spirit of [19], we consider low-rank Tucker approximations of matrix and vector blocks, i.e.

$$\mathbf{A}^{(i,j,k,\ell)} \approx \tilde{\mathbf{A}}^{(i,j,k,\ell)} = \sum_{r_3=1}^{R_3^A} \sum_{r_2=1}^{R_2^A} \sum_{r_1=1}^{R_1^A} \mathfrak{A}_{r_1,r_2,r_3} \tilde{A}_{(3,r_3)}^{(i,j,k,\ell)} \otimes \tilde{A}_{(2,r_2)}^{(i,j,k,\ell)} \otimes \tilde{A}_{(1,r_1)}^{(i,j,k,\ell)}, \quad (3.4)$$

$$\mathbf{f}^{(i,k)} \approx \tilde{\mathbf{f}}^{(i,k)} = \sum_{r_3=1}^{R_3^f} \sum_{r_2=1}^{R_2^f} \sum_{r_1=1}^{R_1^f} \mathfrak{f}_{r_1,r_2,r_3} \tilde{f}_{(3,r_3)}^{(i,k)} \otimes f_{(2,r_2)}^{(i,k)} \otimes f_{(1,r_1)}^{(i,k)}, \quad (3.5)$$

for $i, j = 1, \dots, \mathcal{N}_{sub}$, $k, \ell = 1, 2, 3$, where $R_d^A = R_d^A(i, j, k, \ell)$ and $R_d^f = R_d^f(i, k)$ for $d = 1, 2, 3$. In Section 3.4 we give details on how these approximations can be performed, when the subdomains are defined as unions of neighboring patches.

We collect all the newly defined matrix blocks $\tilde{\mathbf{A}}^{(i,j,k,\ell)}$ and vector blocks $\tilde{\mathbf{f}}^{(i,k)}$ into a single matrix $\tilde{\mathbf{A}}$ and a single vector $\tilde{\mathbf{f}}$, respectively. Then we look for a vector $\tilde{\mathbf{u}}$ with blocks in Tucker format that approximately solves the linear system

$$\tilde{\mathbf{A}}\tilde{\mathbf{u}} = \tilde{\mathbf{f}}.$$

Following [19], we tackle the above problem using a variant of the Truncated Preconditioned Conjugate Gradient (TPCG) method [16, 25]. This is similar to the standard Preconditioned Conjugate Gradient, but after each step truncation is applied to the vector blocks in order keep their ranks sufficiently small.

3.2 The preconditioner

As an “ideal” preconditioner for $\tilde{\mathbf{A}}$ we consider the block diagonal matrix

$$\mathbf{P} = \begin{bmatrix} \mathbf{P}^{(1)} & 0 & \dots & 0 \\ 0 & \mathbf{P}^{(2)} & \dots & 0 \\ \vdots & \vdots & \ddots & \vdots \\ 0 & 0 & \dots & \mathbf{P}^{(\mathcal{N}_{sub})} \end{bmatrix},$$

where for each $i = 1, \dots, \mathcal{N}_{sub}$, $\tilde{\mathbf{P}}^{(i)}$ is a block diagonal approximation of $\mathbf{A}^{(i,i)}$, i.e.

$$\mathbf{P}^{(i)} = \begin{bmatrix} \mathbf{P}^{(i,1)} & 0 & 0 \\ 0 & \mathbf{P}^{(i,2)} & 0 \\ 0 & 0 & \mathbf{P}^{(i,3)} \end{bmatrix},$$

where $\mathbf{P}^{(i,k)}$ is a preconditioner for $\mathbf{A}^{(i,i,k,k)}$, $k = 1, 2, 3$. More precisely, we choose

$$\mathbf{P}^{(i,k)} = c_1^{(i,k)} M_3^{(i)} \otimes M_2^{(i)} \otimes K_1^{(i)} + c_2^{(i,k)} M_3^{(i)} \otimes K_2^{(i)} \otimes M_1^{(i)} + c_3^{(i,k)} K_3^{(i)} \otimes M_2^{(i)} \otimes M_1^{(i)}, \quad (3.6)$$

where, for $d = 1, 2, 3$, $K_d^{(i)}$ and $M_d^{(i)}$ are respectively the stiffness and mass matrix over the univariate spline space $\hat{\mathcal{S}}_{sub,d}^{(i)}$. Differently from [19], here we introduce some constant coefficients $c_\ell^{(i,k)} \in \mathbb{R}$ that aim to take into account the geometry and the elasticity coefficients, whose choice is discussed below. Note that if $c_\ell^{(i,k)} = 1$ for every $\ell = 1, 2, 3$, then $\mathbf{P}^{(i,k)}$ represents the discretization of the Laplace operator over the spline space $\hat{\mathcal{S}}_{sub,0}^{(i)}$.

In practice, $(\mathbf{P}^{(i,k)})^{-1}$ is approximated with a low-rank Tucker matrix $(\tilde{\mathbf{P}}^{(i,k)})^{-1}$ following the steps described in [19, Section 4.2]. We emphasize in particular that this strategy is not spoiled by the presence of the constant coefficients. A key feature of this approach is that the action of $(\tilde{\mathbf{P}}^{(i,k)})^{-1}$ on a vector can be computed using a variant of the Fast Diagonalization method [17, 23] that exploits the Fast Fourier Transform

(FFT), yielding almost linear complexity. In conclusion, the preconditioner $\tilde{\mathbf{P}}$ is the block diagonal matrix obtained by collecting all matrices $\tilde{\mathbf{P}}^{(i,k)}$, for $i = 1, \dots, \mathcal{N}_{sub}$, $k = 1, 2, 3$.

We now discuss the choice of the constant coefficients $c_\ell^{(i,k)}$ appearing in (3.6). We emphasize that a similar approach was used in [10]. We fix $i \in \{1, \dots, \mathcal{N}_{sub}\}$ and $k \in \{1, 2, 3\}$. Let $v_h \in V_{sub}^{(i)}$ and let \mathbf{v} denote its representing vector. It holds

$$\mathbf{v}^T \mathbf{A}^{(i,i,k,k)} \mathbf{v} = \int_{\Theta(i)} 2\mu \varepsilon(\underline{e}_k v_h) : \varepsilon(\underline{e}_k v_h) + \lambda (\nabla \cdot \underline{e}_k v_h) (\nabla \cdot \underline{e}_k v_h) d\mathbf{x} = \int_{[0,1]^3} \left(\nabla \hat{v}_{sub}^{(i)} \right)^T Q^{(i,k)} \nabla \hat{v}_{sub}^{(i)} d\xi,$$

where $\hat{v}_{sub}^{(i)} = v_h \circ \mathcal{G}_i \in \hat{\mathcal{S}}_{sub,0}^{(i)}$, and

$$Q^{(i,k)} = |\det(J_{\mathcal{G}_i})| J_{\mathcal{G}_i}^{-1} \left[\mu (I_3 + \underline{e}_k \underline{e}_k^T) + \lambda \underline{e}_k \underline{e}_k^T \right] J_{\mathcal{G}_i}^{-T}.$$

Here I_3 denotes the 3×3 identity matrix. Moreover,

$$\mathbf{v}^T \mathbf{P}^{(i,k)} \mathbf{v} = \int_{[0,1]^3} \left(\nabla \hat{v}_{sub}^{(i)} \right)^T \begin{bmatrix} c_1^{(i,k)} & 0 & 0 \\ 0 & c_2^{(i,k)} & 0 \\ 0 & 0 & c_3^{(i,k)} \end{bmatrix} \nabla \hat{v}_{sub}^{(i)} d\xi.$$

It is apparent that the 3×3 constant matrix appearing in the above formula should be chosen as the best constant diagonal approximation of $Q^{(i,k)}$. It is therefore reasonable to require that

$$c_\ell^{(i,k)} \approx Q_{\ell,\ell}^{(i,k)}(\xi_1, \xi_2, \xi_3), \quad \ell = 1, 2, 3, \quad \xi_1, \xi_2, \xi_3 \in [0, 1].$$

For example, for $\ell = 1, 2, 3$, we can choose $c_\ell^{(i,k)}$ as the average of $Q_{\ell,\ell}^{(i,k)}$ evaluated on a coarse grid of points.

3.3 The TPCG method with block-wise truncation

As already mentioned, a crucial feature of the TPCG method is the truncation step. Indeed, the operations performed during the iterative process, namely the vector sums and more importantly the matrix-vector products, increase the multilinear ranks of the iterates. Therefore, it is of paramount importance to keep their rank reasonably small through truncation. We emphasize that in our version of the TPCG method the involved vectors (and matrices) do not have a global Tucker structure. Instead, they can be subdivided into blocks with Tucker structure, each with its own multilinear rank. Therefore, all the operations that exploit the Tucker structure, including truncation, are performed to each matrix/vector block separately.

The simplest truncation operator considered here is relative truncation and it is denoted with \mathbf{T}^{rel} . Given Tucker vector \mathbf{v} and a relative tolerance $\epsilon > 0$, $\tilde{\mathbf{v}} = \mathbf{T}^{\text{rel}}(\mathbf{v}, \eta)$ is a Tucker vector with smaller or equal multilinear rank (in each direction) such that

$$\|\tilde{\mathbf{v}} - \mathbf{v}\|_2 \leq \eta \|\mathbf{v}\|_2. \quad (3.7)$$

We refer to [19, Section 4.1.1] for more details.

We also consider a dynamic truncation operator \mathbf{T}^{dt} , which is used only for the approximate solution \mathbf{u}_{k+1} . Here a truncated approximation $\tilde{\mathbf{u}}_{k+1}$ of \mathbf{u}_{k+1} is initially computed using block-wise relative truncation with a prescribed initial tolerance ϵ . Then the algorithm assesses how much the exact solution update $\Delta \mathbf{u}_k = \mathbf{u}_{k+1} - \mathbf{u}_k$ differs from the truncated one $\Delta \tilde{\mathbf{u}}_k = \tilde{\mathbf{u}}_{k+1} - \mathbf{u}_k$ by checking if the condition

$$\left| \frac{\Delta \tilde{\mathbf{u}}_k \cdot \Delta \mathbf{u}_k}{\|\Delta \mathbf{u}_k\|_2^2} - 1 \right| \leq \delta$$

is satisfied, where $\delta > 0$ is a prescribed tolerance. If the condition is satisfied, then $\tilde{\mathbf{u}}_{k+1}$ is accepted as the next iterate. Otherwise, a new tolerance for the relative truncation is selected, equal to $\max\{\alpha\epsilon, \epsilon_{\min}\}$, where $0 < \alpha < 1$ and $\epsilon_{\min} > 0$ is a fixed minimum tolerance. The process is repeated until an acceptable truncated solution is found (or until the tolerance reaches ϵ_{\min}). The final relative tolerance is returned and it is used as initial tolerance for \mathbf{T}^{dt} at the next TPCG iteration. A starting relative tolerance ϵ_0 is fixed at the beginning of the TPCG algorithm. We refer to [19, Section 4.1.2] for more details.

Except for $\tilde{\mathbf{u}}_{k+1}$, all other vectors are compressed using block-wise relative truncation with tolerance

$$\eta_k = \beta \text{tol} \frac{\|\mathbf{r}_0\|_2}{\|\mathbf{r}_k\|_2},$$

where \mathbf{r}_0 and \mathbf{r}_k are the initial and k -th residual vector, respectively, $0 < \beta < 1$ and tol is the TPCG tolerance. This choice of the tolerance promotes low rank, see also [24, 21]. Furthermore, we introduce intermediate truncation steps during the computation of matrix-vector products with $\tilde{\mathbf{A}}$, motivated by the significant rank increment yielded by this operation. We remark, however, that intermediate truncation can lead to cancellation errors and stagnation, see e.g. the discussion in [25, Section 3.6.3]. Therefore, a strict relative tolerance γ should be chosen to safely perform this step.

The TPCG method is reported in Algorithm 1, while Algorithm 2 and Algorithm 3 perform respectively the matrix-vector products with the system matrix (and possibly the computation of the residual) and the application of the preconditioner. Note that, in the latter algorithms, each vector block is truncated immediately after being computed (for Algorithm 2, this is done in addition to the intermediate truncation steps discussed above).

Remark 1. *If the magnitude of the solution changes significantly when different subdomains are considered, it could be a good idea to choose the truncation tolerance for a given vector block basing on the magnitude of the whole vector, as this would help in balancing the error among different subdomains. Consider a vector block $\mathbf{y}^{(i,k)}$, belonging to a vector \mathbf{y} . Its truncation $\tilde{\mathbf{y}}^{(i,k)}$ could be chosen by imposing a condition of the form*

$$\|\tilde{\mathbf{y}}^{(i,k)} - \mathbf{y}^{(i,k)}\|_2 \leq \frac{\eta}{\mathcal{N}_{\text{sub}}} \|\mathbf{y}\|_2,$$

for a given $\eta > 0$ independent of $i \in \{1, \dots, \mathcal{N}_{\text{sub}}\}$, and $k \in \{1, 2, 3\}$. In the present paper we do not use this strategy since for all problems considered in Section 4, the solution is not significantly larger on a portion of the domain with respect to the rest.

Algorithm 1 TPCG

Input: System matrix $\tilde{\mathbf{A}}$ and block diagonal preconditioner $\tilde{\mathbf{P}}$ in block-wise Tucker format, right-hand side \mathbf{f} and initial guess \mathbf{u}_0 in block-wise Tucker format, TPCG tolerance $\text{tol} > 0$, parameter β for the relative truncation, intermediate relative truncation tolerance γ , parameters for the dynamic truncation: starting relative tolerance ϵ_0 , reducing factor α , minimum tolerance ϵ_{\min} , threshold δ .

Output: Low-rank solution $\tilde{\mathbf{u}}$ of $\tilde{\mathbf{A}}\tilde{\mathbf{u}} = \mathbf{f}$.

```

1:  $\eta_0 = \beta \text{tol}$ ;
2:  $\mathbf{r}_0 = -\text{Matvec}(\tilde{\mathbf{A}}, \mathbf{u}_0, \mathbf{f}, \eta_0)$ 
3:  $\mathbf{z}_0 = \text{Prec}(\tilde{\mathbf{P}}, \mathbf{r}_0, \eta_0)$ ;
4:  $\mathbf{p}_0 = \mathbf{z}_0$ ;
5:  $k = 0$ 
6: while  $\|\mathbf{r}_k\|_2 > \text{tol}$  do
7:    $\mathbf{q}_k = \text{Matvec}(\tilde{\mathbf{A}}, \mathbf{p}_k, \mathbf{0}, \gamma, \eta_k)$ ;
8:    $\xi_k = \mathbf{p}_k \cdot \mathbf{q}_k$ 
9:    $\omega_k = \frac{\mathbf{r}_k \cdot \mathbf{p}_k}{\xi_k}$ ;
10:   $[\mathbf{u}_{k+1}, \epsilon_{k+1}] = \text{T}^{\text{dt}}(\mathbf{u}_k, \mathbf{u}_k + \omega_k \mathbf{p}_k, \epsilon_k, \alpha, \epsilon_{\min}, \delta)$ ;
11:   $\mathbf{r}_{k+1} = -\text{Matvec}(\tilde{\mathbf{A}}, \mathbf{u}_{k+1}, \mathbf{f}, \gamma, \eta_k)$ 
12:   $\eta_{k+1} = \beta \text{tol} \frac{\|\mathbf{r}_0\|_2}{\|\mathbf{r}_{k+1}\|_2}$ ;
13:   $\mathbf{z}_{k+1} = \text{Prec}(\tilde{\mathbf{P}}, \mathbf{r}_{k+1}, \eta_{k+1})$ ;
14:   $\beta_k = -\frac{\mathbf{z}_{k+1} \cdot \mathbf{q}_k}{\xi_k}$ ;
15:   $\mathbf{p}_{k+1} = \text{T}^{\text{rel}}(\mathbf{z}_{k+1} + \beta_k \mathbf{p}_k, \eta_{k+1})$ ;
16:   $k = k + 1$ ;
17: end while
18:  $\tilde{\mathbf{u}} = \mathbf{u}_k$ .
```

Algorithm 2 Matvec

Input: Matrix $\tilde{\mathbf{A}}$ in block-wise Tucker format, vectors \mathbf{x} and \mathbf{b} in block-wise Tucker format, intermediate and final relative truncation tolerances γ and η

Output: vector $\tilde{\mathbf{y}}$, block-wise truncation of $\mathbf{y} = \tilde{\mathbf{A}}\mathbf{x} - \mathbf{b}$

```

1: for  $i = 1, \dots, \mathcal{N}_{sub}$  do
2:   for  $k = 1, 2, 3$  do
3:      $\tilde{\mathbf{y}}^{(i,k)} = -\mathbf{b}^{(i,k)}$ 
4:     for  $j = 1, \dots, \mathcal{N}_{sub}$  do
5:       for  $\ell = 1, 2, 3$  do
6:          $\tilde{\mathbf{y}}^{(i,k)} = \text{Trel} \left( \tilde{\mathbf{y}}^{(i,k)} + \tilde{\mathbf{A}}^{(i,j,k,\ell)} \mathbf{x}^{(j,\ell)}, \gamma \right)$ 
7:       end for
8:     end for
9:      $\tilde{\mathbf{y}}^{(i,k)} = \text{Trel} \left( \tilde{\mathbf{y}}^{(i,k)}, \eta \right)$ 
10:  end for
11: end for

```

Algorithm 3 Prec

Input: Block diagonal preconditioner $\tilde{\mathbf{P}}$ with blocks in Tucker format, vector \mathbf{r} in block-wise Tucker format, relative truncation tolerance η

Output: vector $\tilde{\mathbf{z}}$, block-wise truncation of $\mathbf{z} = \tilde{\mathbf{P}}^{-1}\mathbf{r}$

```

1: for  $i = 1, \dots, \mathcal{N}_{sub}$  do
2:   for  $k = 1, 2, 3$  do
3:      $\tilde{\mathbf{z}}^{(i,k)} = \text{Trel} \left( \left( \tilde{\mathbf{P}}^{(i,k)} \right)^{-1} \mathbf{z}^{(i,k)}, \eta \right)$ 
4:   end for
5: end for

```

3.4 Subdomains as unions of patches

In the setting described in Section 2.2, we can choose the subdomains as unions of pairs of patches sharing a face. More precisely, for each face shared by two patches, we introduce a subdomain defined as the union of those patches. Note that in this case \mathcal{N}_{sub} is equal to the number of faces belonging to the interface Γ .

We fix $i \in \{1, \dots, \mathcal{N}_{sub}\}$ and let $i_1, i_2 \in \{1, \dots, \mathcal{N}_{ptc}\}$ such that $\Theta^{(i)} = \Omega^{(i_1)} \cup \Omega^{(i_2)}$. We assume that if a face of $\Omega^{(i_1)}$ shares an edge with a face of $\Omega^{(i_2)}$, then either both faces belong to $\Gamma \cup \partial\Omega_D$, or they both belong to $\partial\Omega_N$. This assumption guarantees that the space obtained by “merging” $V_{ptc}^{(i_1)}$ and $V_{ptc}^{(i_2)}$ can be written as (the pushforward of) a tensor product spline space. Below we give the details.

It is not restrictive to assume that $\Omega^{(i_1)}$ and $\Omega^{(i_2)}$ are attached along the third parametric direction, and in particular that

$$\mathcal{F}_{(i_1)}(\xi_1, \xi_2, 1) = \mathcal{F}_{(i_2)}(\xi_1, \xi_2, 0), \quad (\xi_1, \xi_2) \in [0, 1]^2.$$

Because of the patch conformity assumption, the parametric spline spaces $\hat{\mathcal{S}}_{ptc}^{(i_1)}$ and $\hat{\mathcal{S}}_{ptc}^{(i_2)}$ must have the same knot vectors in the first 2 directions, i.e. $\Xi_1^{(i_1)} = \Xi_1^{(i_2)} =: \Xi_1$ and $\Xi_2^{(i_1)} = \Xi_2^{(i_2)} =: \Xi_2$. Moreover, we consider the knot vectors in the third directions

$$\Xi_3^{(i_1)} = \left\{ \underbrace{0, \dots, 0}_{p+1}, \xi_{p+2}^{(i_1)}, \dots, \xi_{m_3^{(i_1)}}^{(i_1)}, \underbrace{1, \dots, 1}_{p+1} \right\}, \quad \Xi_3^{(i_2)} = \left\{ \underbrace{0, \dots, 0}_{p+1}, \xi_{p+2}^{(i_2)}, \dots, \xi_{m_3^{(i_2)}}^{(i_2)}, \underbrace{1, \dots, 1}_{p+1} \right\}.$$

We now define the “merged” spline space $\hat{\mathcal{S}}_{sub}^{(i)}$, generated by the knot vectors Ξ_1 , Ξ_2 and

$$\Xi_3 = \left\{ \underbrace{0, \dots, 0}_{p+1}, \frac{1}{2}\xi_{p+2}^{(i_1)}, \dots, \frac{1}{2}\xi_{m_3^{(i_1)}}^{(i_1)}, \underbrace{\frac{1}{2}, \dots, \frac{1}{2}}_p, \frac{1}{2}\xi_{p+2}^{(i_2)} + \frac{1}{2}, \dots, \frac{1}{2}\xi_{m_3^{(i_2)}}^{(i_2)} + \frac{1}{2}, \underbrace{1, \dots, 1}_{p+1} \right\} \dots$$

We also consider the geometry mapping $\mathcal{G}_i : [0, 1]^3 \rightarrow \Theta^{(i)}$

$$\mathcal{G}_i(\xi_1, \xi_2, \xi_3) = \begin{cases} \mathcal{F}_{i_1}(\xi_1, \xi_2, 2\xi_3) & \text{if } 0 \leq \xi_3 \leq \frac{1}{2} \\ \mathcal{F}_{i_2}(\xi_1, \xi_2, 2\xi_3 - 1) & \text{if } \frac{1}{2} < \xi_3 \leq 1 \end{cases}. \quad (3.8)$$

We introduce the subspace $\widehat{\mathcal{S}}_{sub,0}^{(j)} \subseteq \widehat{\mathcal{S}}_{sub}^{(j)}$ generated by the basis functions of $\widehat{\mathcal{S}}_{sub}^{(j)}$ whose image through \mathcal{G}_j vanishes on $\Gamma \cup \partial\Omega_D$. We emphasize that, under the aforementioned assumptions on the boundary conditions, $\widehat{\mathcal{S}}_{sub,0}^{(i)}$ is a tensor product space as in (3.2). It holds

$$V_{sub}^{(i)} = \left\{ \hat{v}_h \circ \mathcal{G}_i^{-1} \mid \hat{v}_h \in \widehat{\mathcal{S}}_{sub,0}^{(i)} \right\}.$$

Remark 2. In the case of arbitrary boundary conditions, merging two local spline spaces does not necessarily results in a space which is the pushforward of a tensor product spline space. In this case, one can define $V_{sub}^{(i)}$ by substituting any Neumann boundary conditions with homogenous Dirichlet. Then an additional subdomain should be introduced containing the Neumann degrees of freedom.

We now discuss in detail how the approximations (3.4) and (3.5) can be performed using low-rank techniques. We first consider the case of a matrix block $\mathbf{A}^{(i,j)}$ for $i \neq j$, $i, j \in \{1, \dots, \mathcal{N}_{sub}\}$. Of course if $\Theta^{(i)} \cap \Theta^{(j)}$ has an empty interior, then $\mathbf{A}^{(i,j)}$ is a null matrix. On the other hand, if $\Theta^{(i)} \cap \Theta^{(j)}$ has a non-empty interior, then there is an index $m = m(i, j) \in \{1, \dots, \mathcal{N}_{ptc}\}$ such that $\Theta^{(i)} \cap \Theta^{(j)} = \Omega^{(m)}$. Let $v_h \in V_{sub}^{(i)}$ and $w_h \in V_{sub}^{(j)}$, and let \mathbf{v} and \mathbf{w} be their vector representations. Then for $k, \ell = 1, 2, 3$, it holds

$$\begin{aligned} \mathbf{v}^T \mathbf{A}^{(i,j,k,\ell)} \mathbf{w} &= \int_{\Omega^{(m)}} 2\mu \varepsilon(\underline{e}_k v_h) : \varepsilon(\underline{e}_\ell w_h) + \lambda (\nabla \cdot \underline{e}_k v_h) (\nabla \cdot \underline{e}_\ell w_h) d\underline{x} = \\ &= \int_{[0,1]^3} \left(\nabla \hat{v}_{ptc}^{(m)} \right)^T C^{(m,k,\ell)} \nabla \hat{w}_{ptc}^{(m)} d\underline{\xi}, \end{aligned} \quad (3.9)$$

where $\hat{v}_{ptc}^{(m)} = v_h \circ \mathcal{F}_m$, $\hat{w}_{ptc}^{(m)} = w_h \circ \mathcal{F}_m$, and

$$C^{(m,k,\ell)} = |\det(J_{\mathcal{F}_m})| J_{\mathcal{F}_m}^{-1} \left[\mu (\delta_{k,\ell} I_3 + \underline{e}_\ell \underline{e}_k^T) + \lambda \underline{e}_k \underline{e}_\ell^T \right] J_{\mathcal{F}_m}^{-T}.$$

Here $\delta_{k,\ell}$ is the Kronecker delta. Note that $\hat{v}_{ptc}^{(m)}, \hat{w}_{ptc}^{(m)} \in \widehat{\mathcal{S}}_{ptc,0}^{(m)}$. Moreover, if $\text{supp}(v_h) \cap \Omega^{(m)}$ (respectively $\text{supp}(w_h) \cap \Omega^{(m)}$) has an empty interior then $\hat{v}_{ptc}^{(m)}$ (respectively $\hat{w}_{ptc}^{(m)}$) is the null function and $\mathbf{v}^T \mathbf{A}^{(i,j,k,\ell)} \mathbf{w} = 0$.

We consider a low-rank approximation of the entries of $C^{(m,k,\ell)}$:

$$C_{\alpha,\beta}^{(m,k,\ell)}(\xi_1, \xi_2, \xi_3) \approx \sum_{r_1, r_2, r_3} \mathbf{c}_{r_1, r_2, r_3}^{(m,k,\ell,\alpha,\beta)} \cdot c_{1,r_1}^{(m,k,\ell,\alpha,\beta)}(\xi_1) \cdot c_{2,r_2}^{(m,k,\ell,\alpha,\beta)}(\xi_2) \cdot c_{3,r_3}^{(m,k,\ell,\alpha,\beta)}(\xi_3). \quad (3.10)$$

Plugging (3.10) into (3.9), we obtain

$$\mathbf{v}^T \mathbf{A}^{(i,j,k,\ell)} \mathbf{w} \approx \sum_{r_1, r_2, r_3} \sum_{\alpha, \beta=1}^3 \mathbf{c}_{r_1, r_2, r_3}^{(m,k,\ell,\alpha,\beta)} \int_{[0,1]^3} c_{1,r_1}^{(m,k,\ell,\alpha,\beta)} c_{2,r_2}^{(m,k,\ell,\alpha,\beta)} c_{3,r_3}^{(m,k,\ell,\alpha,\beta)} \partial_\alpha \hat{v}_{ptc}^{(m)} \partial_\beta \hat{w}_{ptc}^{(m)} d\underline{\xi}.$$

Therefore, thanks to the tensor structure of the spline space $\widehat{\mathcal{S}}_{ptc,0}^{(m)}$ the matrix block $\mathbf{A}^{(i,j,k,\ell)}$ can be approximated as

$$\mathbf{A}^{(i,j,k,\ell)} \approx \sum_{r_1, r_2, r_3} \sum_{\alpha, \beta=1}^3 \mathbf{c}_{r_1, r_2, r_3}^{(m,k,\ell,\alpha,\beta)} \tilde{A}_{3,r_3}^{(i,j,k,\ell,\alpha,\beta)} \otimes \tilde{A}_{2,r_2}^{(i,j,k,\ell,\alpha,\beta)} \otimes \tilde{A}_{1,r_1}^{(i,j,k,\ell,\alpha,\beta)}, \quad (3.11)$$

where each Kronecker factor $\tilde{A}_{d,r_d}^{(i,j,k,\ell,\alpha,\beta)}$ is an $n_{sub,d}^{(i)} \times n_{sub,d}^{(j)}$ matrix with null entries outside of a square $n_{ptc,d}^{(m)} \times n_{ptc,d}^{(m)}$ block $\tilde{A}_{d,r_d}^{(m,k,\ell,\alpha,\beta)}$ whose entries are

$$\left(\tilde{A}_{d,r_d}^{(m,k,\ell,\alpha,\beta)} \right)_{s,t} = \int_0^1 c_{d,r_d}^{(m,k,\ell,\alpha,\beta)}(\xi_d) \left[\hat{b}_{d,s}^{(m)}(\xi_d) \right]^{(d,\alpha)} \left[\hat{b}_{d,t}^{(m)}(\xi_d) \right]^{(d,\beta)} d\xi_d, \quad s, t = 1, \dots, n_{ptc,d}^{(m)},$$

with

$$[f(\xi)]^{(d,\gamma)} = \begin{cases} f'(\xi) & \text{if } d = \gamma \\ f(\xi) & \text{otherwise} \end{cases}, \quad d, \gamma = 1, 2, 3,$$

Note that (3.11) can be easily written in the Tucker format (3.4).

There is of course more than one approach to compute the low-rank approximation (3.10). A suitable possibility, proposed in [18], is to interpolate the left-hand side function using a coarse spline space and then performing a High Order Singular Value Decomposition (HOSVD) [6]. In this work, however, we follow [19] and employ the strategy described in [8, 7], which is based on interpolation with Chebyshev polynomials.

We now discuss the low-rank approximation of a given vector block $\mathbf{f}^{(i,k)}$, where $i \in \{1, \dots, \mathcal{N}_{ptc}\}$, and $k \in \{1, 2, 3\}$. Let $v_h \in V_{sub}^{(i)}$ and let \mathbf{v} be its vector representation. It holds

$$v^T \mathbf{f}^{(i,k)} = \int_{\Theta^{(i)}} f_k(\underline{x}) v_h(\underline{x}) d\underline{x} = \int_{[0,1]^3} \hat{f}_k^{(i)}(\underline{\xi}) \hat{v}_h^{(i)}(\underline{\xi}) d\underline{\xi}, \quad (3.12)$$

where $\hat{f}_k^{(i)} = \det(J_{\mathcal{G}_i}) (f_k \circ \mathcal{G}_i^{-1})$ and $\hat{v}_{sub}^{(i)} = v_h \circ \mathcal{G}_i^{-1} \in \hat{\mathcal{S}}_{sub,0}^{(i)}$. We consider a low-rank approximation

$$\hat{f}_k^{(i)}(\xi_1, \xi_2, \xi_3) \approx \sum_{r_1, r_2, r_3} \mathfrak{f}_{r_1, r_2, r_3}^{(i,k)} \cdot f_{(1, r_1)}^{(i,k)}(\xi_1) \cdot f_{(2, r_2)}^{(i,k)}(\xi_2) \cdot f_{(3, r_3)}^{(i,k)}(\xi_3) \quad (3.13)$$

Plugging (3.13) into (3.12) we obtain

$$v^T \mathbf{f}^{(i,k)} \approx \sum_{r_1, r_2, r_3} \mathfrak{f}_{r_1, r_2, r_3}^{(i,k)} \int_{[0,1]^3} f_{(1, r_1)}^{(i,k)}(\xi_1) f_{(2, r_2)}^{(i,k)}(\xi_2) f_{(3, r_3)}^{(i,k)}(\xi_3) \hat{v}_{sub}^{(i)}(\underline{\xi}) d\underline{\xi}.$$

Therefore, thanks to the tensor structure of the spline space $\hat{\mathcal{S}}_{sub,0}^{(i)}$ the vector block $\mathbf{f}^{(i,k)}$ can be approximated as in (3.5).

We now discuss the technical details of the low-rank approximation (3.13) considered in this work. Assuming that \mathcal{G}_i is given by (3.8), we first use the **Chebfun3F** algorithm [7] to independently compute low-rank approximations of $\hat{f}_k^{(i)} = \det(J_{\mathcal{G}_i}) (f_k \circ \mathcal{G}_i^{-1})$ for $0 \leq \xi_3 \leq \frac{1}{2}$ and for $\frac{1}{2} < \xi_3 \leq 1$. The reason for this separation is that $J_{\mathcal{G}_i}$ is possibly discontinuous at $\xi_3 = \frac{1}{2}$ (corresponding to the interface between the two patches in the physical domain) and this could hinder the effectiveness of the considered low-rank Chebyshev approximation. Note that also f_k could be discontinuous. We extend the two approximations of $\hat{f}_k^{(i)}$, denoted with $\tilde{f}_{k,1}^{(i)}$ and $\tilde{f}_{k,2}^{(i)}$, by zero outside of their respective domain. Then we consider

$$\hat{f}_k^{(i)} \approx \tilde{f}_k^{(i)} = \tilde{f}_{k,1}^{(i)} + \tilde{f}_{k,2}^{(i)}.$$

Note that the multilinear rank of $\tilde{f}_k^{(i)}$ is given by the sum of the multilinear ranks of $\tilde{f}_{k,1}^{(i)}$ and $\tilde{f}_{k,2}^{(i)}$. As a final step, we reduce the rank of the approximation using a purely algebraic approach based on the HOSVD.

We finally briefly discuss the Tucker approximation of a given matrix block $\mathbf{A}^{(i,i,k,\ell)}$, where $i \in \{1, \dots, \mathcal{N}_{sub}\}$, $k, \ell \in \{1, 2, 3\}$. Let $v_h, w_h \in V_{sub}^{(i)}$, and let \mathbf{v} and \mathbf{w} be their vector representations. It holds

$$\begin{aligned} \mathbf{v}^T \mathbf{A}^{(i,i,k,\ell)} \mathbf{w} &= \int_{\Theta^{(i)}} 2\mu \varepsilon(\underline{e}_k v_h) : \varepsilon(\underline{e}_\ell w_h) + \lambda (\nabla \cdot \underline{e}_k v_h) (\nabla \cdot \underline{e}_\ell w_h) d\underline{x} = \\ &= \int_{[0,1]^3} \left(\nabla \hat{v}_{sub}^{(i)} \right)^T Q^{(i,k,\ell)} \nabla \hat{w}_{sub}^{(i)} d\underline{\xi}, \end{aligned} \quad (3.14)$$

where $\hat{v}_{sub}^{(i)} = v_h \circ \mathcal{G}_i$, $\hat{w}_{sub}^{(i)} = w_h \circ \mathcal{G}_i \in \hat{\mathcal{S}}_{sub,0}^{(i)}$, and

$$Q^{(i,k,\ell)} = |\det(J_{\mathcal{G}_i})| J_{\mathcal{G}_i}^{-1} [\mu (\delta_{k,\ell} I_3 + \underline{e}_\ell \underline{e}_k^T) + \lambda \underline{e}_k \underline{e}_\ell^T] J_{\mathcal{G}_i}^{-T}.$$

We consider the following low-rank approximations of the entries of $Q^{(i,k,\ell)}$:

$$Q_{\alpha,\beta}^{(i,k,\ell)}(\xi_1, \xi_2, \xi_3) \approx \sum_{r_1, r_2, r_3} \mathbf{q}_{r_1, r_2, r_3}^{(i,k,\ell,\alpha,\beta)} \cdot q_{1,r_1}^{(i,k,\ell,\alpha,\beta)}(\xi_1) \cdot q_{2,r_2}^{(i,k,\ell,\alpha,\beta)}(\xi_2) \cdot q_{3,r_3}^{(i,k,\ell,\alpha,\beta)}(\xi_3). \quad (3.15)$$

This approximation can be computed using the same strategy as for (3.13). Plugging (3.15) into (3.14), and exploiting the tensor structure of $\hat{\mathcal{S}}_{sub,0}^{(i)}$, we obtain the Tucker approximation (3.4).

4 Numerical experiments

In this section we present some numerical experiments to show the behavior of our low-rank solving strategy for multipatch geometries. All the tests are performed with Matlab R2022b on an Intel(R) Core(TM) i9-12900K, running at 3.20 GHz, and with 128 GB of RAM.

We used GeoPDEs toolbox [26] to handle isogeometric discretizations. The approximation of the right-hand side and the linear system matrix are computed using Chebfun toolbox functions [8].

In all the tests, we employ a dyadic refinement and every patch has the same number of elements $n_{el} = 2^L$ in each parametric direction and for different discretization levels L . The numerical solution is computed with the TPCG method, discussed in Section 3.3, with relative tolerance $tol = 10^{-6}$ and the zero vector as initial guess. The system matrix and the right-hand side are approximated with the technique of Section 3.4 by setting the relative tolerance of **Chebfun3F** equal to $10^{-1}tol = 10^{-7}$ (see [7] for more details). The dynamic truncation described in Section 3.3 is used fixing the initial relative tolerance as $\epsilon_0 = 10^{-1}$ and the minimum relative tolerance as $\epsilon_{\min} = tol\|\mathbf{f}\|_2 10^{-1}$. The threshold δ is set equal to 10^{-3} , the reducing factor α is set equal to 0.5. The relative tolerance parameter β is chosen as 10^{-1} , while the intermediate relative tolerance γ is chosen as 10^{-8} . The relative tolerance ϵ_{rel}^{prec} for the approximation of the diagonal blocks of the preconditioner (see [19] for details) is set equal to 10^{-1} . We experimentally verified that these choices of the parameters yield good performance of the TPCG method.

We set the right-hand side equal to $\underline{\mathbf{f}} = [0, 0, -0.3]^T$ and the Lamé parameters equal to $\lambda = \frac{0.3}{0.52}$ and $\mu = \frac{1}{2.6}$ (these values correspond to the choice $E = 1$ for the young modulus and $\nu = 0.3$ for the Poisson's ratio). Let

$$\tilde{\mathbf{u}}^{(j)} := \begin{bmatrix} \tilde{\mathbf{u}}^{(j,1)} \\ \tilde{\mathbf{u}}^{(j,2)} \\ \tilde{\mathbf{u}}^{(j,3)} \end{bmatrix}, \quad j = 1, \dots, \mathcal{N}_{sub}$$

be the solution of the linear elasticity problem in Tucker format in each subdomain. We denote with $(R_1^{\mathbf{u}}(j, d), R_2^{\mathbf{u}}(j, d), R_3^{\mathbf{u}}(j, d))$ the multilinear rank of $\tilde{\mathbf{u}}^{(j,d)}$, for $d = 1, 2, 3$ and $j = 1, \dots, \mathcal{N}_{sub}$. The memory compression percentage of the low-rank solution with respect to the full solution is defined as

$$\text{memory compression} := \frac{\sum_{j=1}^{\mathcal{N}_{sub}} \sum_{d=1}^3 \left(R_1^{\mathbf{u}}(j, d) n_{sub,1}^{(j)} + R_2^{\mathbf{u}}(j, d) n_{sub,2}^{(j)} + R_3^{\mathbf{u}}(j, d) n_{sub,3}^{(j)} \right)}{N_{dof}} \cdot 100, \quad (4.1)$$

where $N_{dof} := \sum_{j=1}^{\mathcal{N}_{sub}} n_{sub,1}^{(j)} n_{sub,2}^{(j)} n_{sub,3}^{(j)}$ represents the total number of degrees of freedom, i.e. the dimension of the space $\sum_{j=1}^{\mathcal{N}_{sub}} V_{sub}^{(j)}$. Note that we only consider the memory compression of the solution and not the memory compression of the right-hand side and of the linear system matrix, that has already been analyzed in [18, 12, 3].

In the numerical experiments we show the maximum of the multilinear rank of all the components of the solution. Thanks to the strategy employed for the truncation of the iterates $\mathbf{r}_k, \mathbf{z}_k, \mathbf{p}_k$ and \mathbf{q}_k , the maxima of their multilinear ranks is comparable to the one of \mathbf{u}_k when convergence approaches, and thus their values are not reported.

4.1 L-shaped domain

In this test we consider a three dimensional L-shaped domain, as represented in Figure 1a, where different colors represent different patches. We have two subdomains, one is the union of the yellow and light green patches and the other the union of the light green and dark green patches. We consider homogeneous Dirichlet boundary conditions on the patch faces that lie on the planes $\{x = -1\} \cup \{z = 1\} \cup \{x = 0\} \cup \{z = 0\}$, and homogeneous Neumann boundary conditions elsewhere. The solution is represented in Figure 1b.

For this domain, the multilinear ranks of the blocks of $\tilde{\mathbf{A}}$ (note that here the geometry is trivial for all patches, therefore $\mathbf{A} = \tilde{\mathbf{A}}$) are

$$(R_1^{\mathbf{A}}(i, j, k, k), R_2^{\mathbf{A}}(i, j, k, \ell), R_3^{\mathbf{A}}(i, j, k, \ell)) = (3, 3, 3), \quad k = 1, 2, 3,$$

and

$$(R_1^{\mathbf{A}}(i, j, k, \ell), R_2^{\mathbf{A}}(i, j, k, \ell), R_3^{\mathbf{A}}(i, j, k, \ell)) = (2, 2, 2), \quad k, \ell = 1, 2, 3, k \neq \ell,$$

for $i, j = 1, 2$.

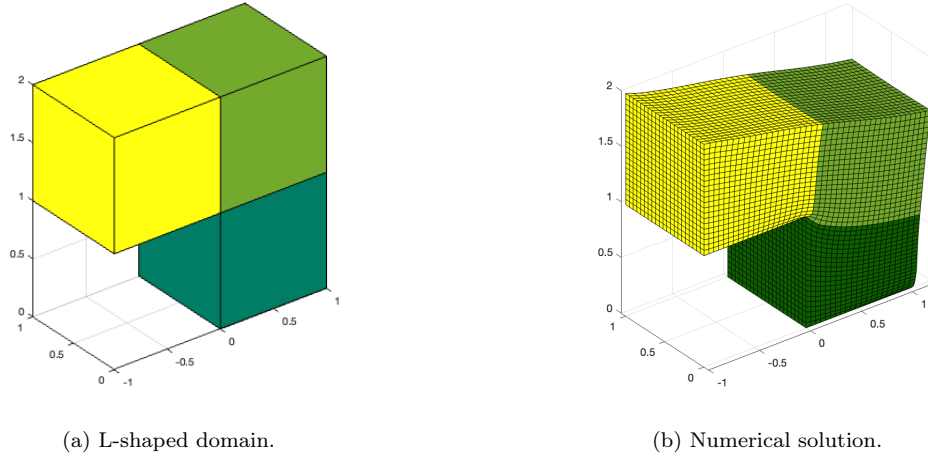


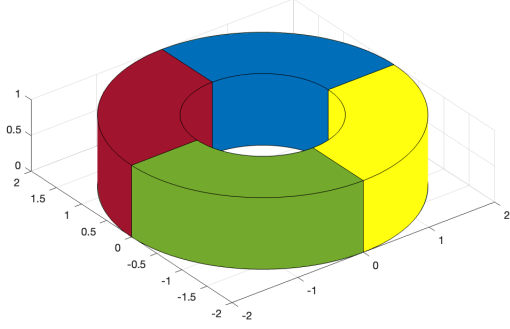
Figure 1: Initial domain and numerical solution of the L-shaped domain.

In Table 1 we report the number of iterations for degrees $p = 2, 3, 4, 5$ and number of elements per patch per parametric direction $n_{el} = 2^L$ with $L = 5, \dots, 8$. The number of iterations is almost independent of the degree and grows only mildly with the number of elements n_{el} . We emphasize that for the finer discretization level the number of degrees of freedom is roughly 200 millions.

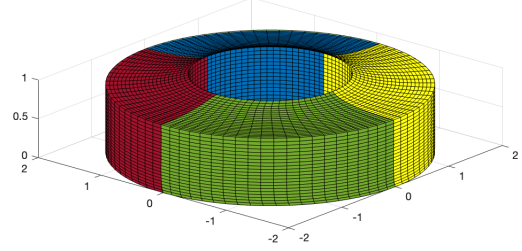
	Iteration number			
n_{el}	$p = 2$	$p = 3$	$p = 4$	$p = 5$
32	34	36	34	35
64	37	38	36	37
128	43	42	40	41
256	52	51	48	49

Table 1: Number of iterations for the L-shaped domain.

Figure 2a shows the maximum of the multilinear ranks of the solution in all the displacement directions and in all the subdomains: the ranks grow as the degree and number of elements is increased, implying that the solution has not a low-rank. The memory compression (4.1), represented in Figure 2b, highlights the great memory saving that we have with the multipatch low-rank strategy with respect to the full one. Note that the maximum rank of the solution is rather large, between 100 and 150 on the finest discretization level. Nevertheless, the memory compression is around 1% for this level.

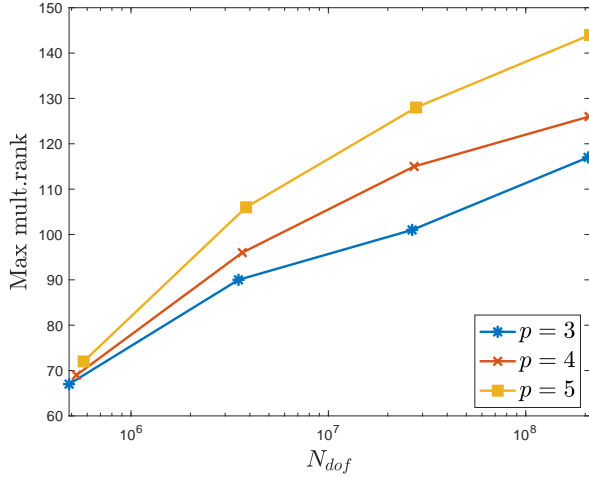


(a) Ring domain.

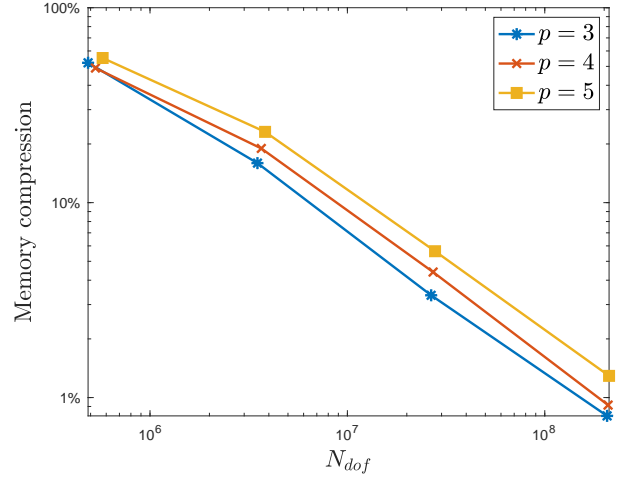


(b) Numerical solution.

Figure 3: Initial domain and numerical solution of the ring domain.



(a) Maximum of the multilinear rank of the solution.



(b) Memory compression.

Figure 2: Results for the L-shaped domain.

4.2 Ring domain

In this test we consider a thick ring domain, represented in Figure 3a. We have four patches and four subdomains, represented by the union of green and yellow patches, yellow and blue patches, blue and red patches and red and green patches. We impose homogeneous Dirichlet boundary conditions on $\{z = 0\}$ and in the central walls of the ring, while homogeneous Neumann boundary conditions are imposed elsewhere. The numerical solution is represented in Figure 3b.

For this domain, the multilinear ranks of the blocks of $\tilde{\mathbf{A}}$ are

$$(R_1^A(i, j, 1, 1), R_2^A(i, j, 1, 1), R_3^A(i, j, 1, 1)) = (R_1^A(i, j, 2, 2), R_2^A(i, j, 1, 1), R_3^A(i, j, 2, 2)) = (5, 5, 5),$$

$$(R_1^A(i, j, 3, 3), R_2^A(i, j, 3, 3), R_3^A(i, j, 3, 3)) = (3, 3, 3)$$

and

$$(R_1^A(i, j, k, \ell), R_2^A(i, j, k, \ell), R_3^A(i, j, k, \ell)) = (4, 4, 4), \quad k, \ell = 1, 2, 3, k \neq \ell,$$

for $i, j = 1, 2, 3, 4$.

Table 2 collects the number of iterations for degrees $p = 2, 3, 4, 5$ and number of elements per patch per parametric direction $n_{el} = 2^L$ with $L = 5, \dots, 8$, as in the previous test. The number of iterations grows mildly in the number of elements and decreases when p increases.

	Iteration number			
n_{el}	$p = 2$	$p = 3$	$p = 4$	$p = 5$
32	59	42	39	40
64	63	44	41	42
128	71	50	46	46
256	77	60	58	55

Table 2: Number of iterations for the ring domain.

We report in Figure 4a the maximum of the multilinear ranks of the solution in all the directions and for all the subdomains. As in the previous test case, the solution has multilinear ranks that grow when n_{el} increases. Nevertheless, as represented in Figure 4b, the memory storage for the solution is hugely reduced with respect to the full solution and reaches values around 1% for the highest discretization level.

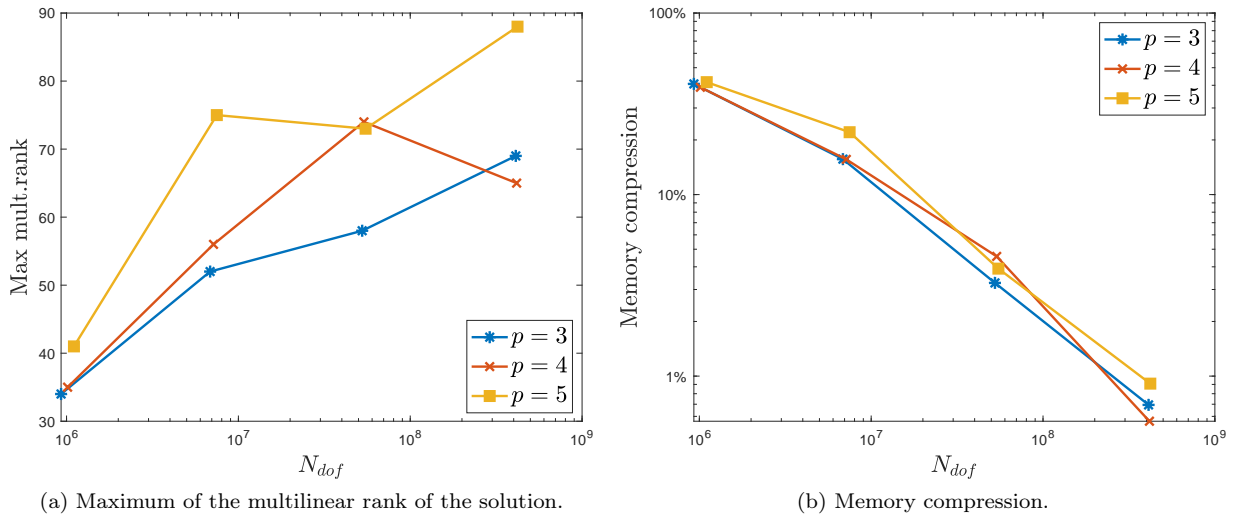


Figure 4: Results for the ring domain.

5 Conclusions

In this work, we have considered the isogeometric discretization of compressible linear elasticity problems. We extended the low-rank solution method first presented [19], which is based on a low-rank Tucker representation of vectors and matrices, to conforming multipatch discretizations.

This non-trivial extension is based on an overlapping Schwarz solver where the subdomains are built from union of pairs of adjoining patches. Each block of the (possibly singular) system matrix and each block of the right hand side vector is approximated by a Tucker matrix and a Tucker vector, respectively. The resulting linear system is solved using the Truncated Preconditioned Conjugate Gradient Method. The designed preconditioner has a block-diagonal structure where each block is a Tucker matrix and its application exploits the Fast Diagonalization method and the Fast Fourier Transform.

We performed numerical tests showing the low memory storage, almost independent of the degree p , and a robust number of iterations with respect to p and the mesh-size.

Acknowledgments

The authors are members of the Gruppo Nazionale Calcolo Scientifico-Istituto Nazionale di Alta Matematica (GNCS-INDAM), the first author was partially supported by INDAM-GNCS Project 2023 “Efficienza ed analisi di metodi numerici innovativi per la risoluzione di PDE”. M. Tani acknowledge the contribution of the Italian Ministry of University and Research (MUR) through the PRIN project COSMIC (No. 2022A79M75). G. Sangalli acknowledges support from PNRR-M4C2-I1.4-NC-HPC-Spoke6.

References

- [1] A. Bressan, M. Martinelli, and G. Sangalli. in preparation.
- [2] A. Bressan and E. Sande. Approximation in FEM, DG and IGA: a theoretical comparison. *Numerische Mathematik*, 2019.
- [3] A. Bünger, S. Dolgov, and M. Stoll. A low-rank tensor method for PDE-constrained optimization with isogeometric analysis. *SIAM Journal on Scientific Computing*, 42(1):A140–A161, 2020.
- [4] J. A. Cottrell, T. J. R. Hughes, and Y. Bazilevs. *Isogeometric analysis: toward integration of CAD and FEA*. John Wiley & Sons, 2009.
- [5] C. De Boor. *A practical guide to splines (revised edition)*. Applied Mathematical Sciences. Springer, 2001.
- [6] L. De Lathauwer, B. De Moor, and J. Vandewalle. A multilinear singular value decomposition. *SIAM journal on Matrix Analysis and Applications*, 21(4):1253–1278, 2000.
- [7] S. Dolgov, D. Kressner, and C. Strossner. Functional Tucker approximation using Chebyshev interpolation. *SIAM Journal on Scientific Computing*, 43(3):A2190–A2210, 2021.
- [8] T. A Driscoll, N. Hale, and L. N. Trefethen. *Chebfun Guide*. Pafnuty Publications, 2014.
- [9] J. A. Evans, Y. Bazilevs, I. Babuška, and T. J. R. Hughes. n -widths, sup-infs, and optimality ratios for the k -version of the isogeometric finite element method. *Computer Methods in Applied Mechanics and Engineering*, 198:1726–1741, 2009.
- [10] J. C. Fuentes, T. Elguedj, D. Dureisseix, and A. Duval. A cheap preconditioner based on fast diagonalization method for matrix-free weighted-quadrature isogeometric analysis applied to nonlinear transient heat transfer problems. *Computer Methods in Applied Mechanics and Engineering*, 414:116157, 2023.
- [11] I. Georgieva and C. Hofreither. Greedy low-rank approximation in Tucker format of solutions of tensor linear systems. *Journal of Computational and Applied Mathematics*, 358:206–220, 2019.
- [12] C. Hofreither. A black-box low-rank approximation algorithm for fast matrix assembly in isogeometric analysis. *Computer Methods in Applied Mechanics and Engineering*, 333:311–330, 2018.
- [13] T. J. R. Hughes, J. A. Cottrell, and Y. Bazilevs. Isogeometric analysis: Cad, finite elements, nurbs, exact geometry and mesh refinement. *Computer methods in applied mechanics and engineering*, 194(39-41):4135–4195, 2005.
- [14] B. Jüttler and D. Mokriš. Low rank interpolation of boundary spline curves. *Computer Aided Geometric Design*, 55:48–68, 2017.
- [15] E. F. Kaasschieter. Preconditioned conjugate gradients for solving singular systems. *Journal of Computational and Applied mathematics*, 24(1-2):265–275, 1988.
- [16] D. Kressner and C. Tobler. Low-rank tensor Krylov subspace methods for parametrized linear systems. *SIAM Journal on Matrix Analysis and Applications*, 32(4):1288–1316, 2011.
- [17] R. E. Lynch, J. R. Rice, and D. H. Thomas. Direct solution of partial difference equations by tensor product methods. *Numerische Mathematik*, 6(1):185–199, 1964.

- [18] A. Mantzaflaris, B. Jüttler, B. N. Khoromskij, and U. Langer. Low rank tensor methods in Galerkin-based isogeometric analysis. *Comput. Methods Appl. Mech. Engrg.*, 316:1062–1085, 2017.
- [19] M. Montardini, G. Sangalli, and M. Tani. A low-rank isogeometric solver based on Tucker tensors. *Comput. Methods Appl. Mech. Engrg.*, page 116472, 2023.
- [20] I. V. Oseledets, D. V. Savostyanov, and E. E. Tyrtyshnikov. Linear algebra for tensor problems. *Computing*, 85(3):169–188, 2009.
- [21] D. Palitta and P. Kürschner. On the convergence of Krylov methods with low-rank truncations. *Numerical Algorithms*, 88(3):1383–1417, 2021.
- [22] M. Pan and F. Chen. Low-rank parameterization of volumetric domains for isogeometric analysis. *Computer-Aided Design*, 114:82–90, 2019.
- [23] G. Sangalli and M. Tani. Isogeometric preconditioners based on fast solvers for the Sylvester equation. *SIAM Journal on Scientific Computing*, 38(6):A3644–A3671, 2016.
- [24] V. Simoncini and D. B. Szyld. Theory of inexact Krylov subspace methods and applications to scientific computing. *SIAM Journal on Scientific Computing*, 25(2):454–477, 2003.
- [25] C. Tobler. *Low-rank tensor methods for linear systems and eigenvalue problems*. PhD thesis, ETH Zurich, 2012.
- [26] R. Vázquez. A new design for the implementation of isogeometric analysis in Octave and Matlab: GeoPDEs 3.0. *Computers & Mathematics with Applications*, 72(3):523–554, 2016.